ISSN 1063-7761, Journal of Experimental and Theoretical Physics, 2017, Vol. 125, No. 5, pp. 798–809. © Pleiades Publishing, Inc., 2017.
Original Russian Text © Yu.S. Orlov, V.A. Dudnikov, 2017, published in Zhurnal Eksperimental'noi i Teoreticheskoi Fiziki, 2017, Vol. 152, No. 5, pp. 944–956.

ORDER, DISORDER, AND PHASE TRANSITION IN CONDENSED SYSTEM

Polaron Model of a Pseudogap State in Quasi-One-Dimensional Systems

Yu. S. Orlov[a,b,*] and V. A. Dudnikov[a]

[a] *Kirensky Institute of Physics, Siberian Branch, Russian Academy of Sciences, Akademgorodok 50/38, Krasnoyarsk, 660036 Russia*

[b] *Siberian Federal University, Krasnoyarsk, 660041 Russia*

**e-mail: jso.krasn@mail.ru*

Received May 8, 2017

Abstract—A brief overview of the basic concepts and problems of the physics of quasi-one-dimensional (q1D) compounds is given. A consistent theoretical description of the nature of the so-called pseudogap state still remains the main problem. A simplified model of the pseudogap state based on the formation of small-radius polarons is considered within the cluster perturbation theory.

DOI: 10.1134/S1063776117110103

1. INTRODUCTION

The scattering of free electrons and holes by optical and acoustic phonons is a first-order effect of perturbation theory with respect to electron–phonon interaction (EPI). At the same time, there is a second-order effect, which is associated with the fact that, in a number of cases, phonons may change the energy spectrum of free charge carriers. This phenomenon is called the polaron effect, and a charge carrier interacting with phonons is called a polaron. Polaron theory is a large field of solid state physics. Today, there is a new surge of activity in this field. First of all, this is associated with the study of high-temperature superconductors, various multiferroics, manganites with colossal magnetoresistance, and quasi-one-dimensional (q1D) systems. Moreover, the recently arisen possibility of modeling and simulation of many polaron phenomena in systems of ultracold atoms in 1D and 2D optical lattices has strongly attracted the attention of researchers, because it allows one to appropriately change the parameters of a physical system [1–3]. To this end, one immerses an optical lattice with carriers (Bose or Fermi atoms) in a Bose–Einstein condensate; as a result of interaction with this condensate, a polaron state is formed in the form of a carrier dressed in a coherent phonon cloud—Bogolyubov excitations [4, 5]. In the present study, we deal only with q1D systems. Below we give basic information and recent results on the study of the electronic structure of q1D systems and outline the main challenges that require solution.

Theoretical investigations of 1D electronic systems, which started long before q1D-type crystals were obtained experimentally, have shown that the properties of electronic 1D systems significantly differ from the properties of crystals with 2D or 3D motion of electrons. The following three statements adequately characterize the whole specifics of 1D systems [6].

(a) A metallic 1D system without Coulomb interaction of electrons is unstable with respect to a periodic potential with wave vector $2k_F$. This instability leads to a self-consistent periodic variation in the electron density and the displacement of lattice atoms and opens a gap in the energy spectrum at the Fermi level. In other words, a decrease in the temperature of a 1D metal should give rise to lattice distortions with wave number equal to twice the Fermi momentum, and the ground state of a 1D chain of atoms at zero temperature is the dielectric state [7]. Such a self-consistent variation in the electron density and the position of lattice atoms is called a charge density wave (CDW).

(b) In a 1D electronic system with a half-filled band, single-electron excitations are separated from the ground state by a gap for an arbitrarily weak repulsion of electrons [8]. This assertion is proved in the case when the electron interaction is described within the framework of the Hubbard Hamiltonian. However, there is no reason to believe that this statement is not correct for the real Coulomb interaction of electrons. Thus, the Coulomb interaction between electrons leads to a dielectric (Mott) transition as temperature decreases.

(c) Single-electron states in a 1D system are localized in an arbitrarily weak random potential. Therefore, at low temperatures, the conductivity of a 1D electronic system in a lattice with defects cannot be metallic [9]. In his now classical work [10], Berezinskii was the first to give a consistent solution to the prob-

lem of localization of electronic states in a one-dimensional system with arbitrarily weak disorder.

All these statements show that a 1D electronic system can be nonmetallic at low temperatures for at least three reasons.

In spite of the fact that q1D conductors with CDWs have not yet found practical application, the diversity and uniqueness of their properties still attract the attention of researchers from different countries [11, 12].

In recent years, great interest has been shown in the study of a pseudogap in the spectrum of elementary excitations in various q1D systems. Pseudogap anomalies were observed in a number of experiments, such as the measurements of optical conductivity, inelastic neutron scattering, and angle-resolved photoemission spectroscopy (ARPES) [13].

Characteristic features of the intensity spectra of an ARPES signal in q1D compounds with CDWs are the shift of the maximum intensity of the spectrum in depth from the Fermi level and its broadening with stronger energy smearing compared with that of conventional 3D quasiparticles in metals at the Fermi level, for which the maximum is described by a Lorentzian. Among inorganic materials, ARPES was applied to blue bronze $K_{0.3}MoO_3$ [14], as well as to $(TaSe_4)_2I$ [15].

According to mean field theory, the density of states for single-particle excitations within the Fröhlich model is described by the inverse square root dependence $dN/dE = D(E) \sim 1/\sqrt{E - 2\Delta}$; however, the spectra of real q1D compounds with density waves hardly ever exhibit inverse square root behavior [16]. Experimental spectra of the density of states are almost always smeared near the energy $E = 2\Delta$ by a value much greater than k_BT [17, 18]. One of the reasons is the strong fluctuations of the order parameter and EPI, which lead to the interaction of free carriers with these fluctuations and give rise to self-localized states. According to modern concepts, fluctuations also lead to a difference between the temperature of the Peierls transition and the value predicted by mean field theory.

The order parameter describing the modulation of CDWs is given by

$$\Delta = g(2k_F)\langle b_{2k_F} + b^+_{-2k_F}\rangle e^{i2k_Fx} = |\Delta|e^{i2k_Fx},$$

where the brackets $\langle ... \rangle$ denote thermodynamic averaging. A gap of 2Δ opens in the electronic spectrum at the Fermi level, and the dispersion of a single-particle excitation becomes

$$E(k) = \mathrm{sgn}\varepsilon(k)[\varepsilon^2(k) + |\Delta|^2]^{1/2}.$$

In this case, just as for superconductivity, the predicted ratio of the Peierls gap to the critical temperature is

$$2\Delta/k_BT_C = 3.52.$$

However, according to numerous experimental data [16, 19, 20], in inorganic q1D conductors, the value of $2\Delta/k_BT_C$ ranges from 8 to 14, depending on the compound; therefore, one distinguishes between the transition temperature in the mean field theory, T_{MF}, and the experimentally determined transition temperature T_P. According to modern concepts, T_P corresponds to the temperature of 3D ordering, T_{3D}, where the interaction between fluctuations of the order parameter of CDWs on neighboring 1D chains (i.e., in a direction perpendicular to the direction of maximum conductivity) gives rise to the correlation of the order parameter in all three directions and a 3D CDW. A theoretical justification is given in [21] by Lee, Rice, and Anderson, who showed that, strictly speaking, the system has no long-range order at any finite temperature, because the correlation function decays exponentially with the distance:

$$\langle \Delta(x)\Delta(0)\rangle \propto \exp(-x/\xi(T)).$$

However, below $T_{3D} \sim T_{MF}/4$, the correlation length $\xi(T)$ diverges exponentially; therefore, one can assume that, at temperatures below $T_{MF}/4$, a Peierls superlattice is formed in the system. Strong fluctuations of the order parameter Δ also exist above T_{3D} and are correlated up to $T^* > T_{3D}$; for $T > T^*$, the correlation length $\xi_\perp$ becomes less than the distance between the chains. The results of calculations show that the system exhibits a dip in the density of states, rather than a gap. Only at temperatures $T < T_{MF}/4$ the density of states approaches the value obtained in the molecular field approximation. A decrease in the transition temperature, obtained in [21], is a result of a compromise between two opposite tendencies: on the one hand, the state with CDWs has the lowest energy for $T < T_{MF}$, while, on the other hand, in a strictly 1D system, long-range order is impossible at finite temperature.

Direct experimental manifestations of fluctuations in q1D conductors are the smearing of X-ray reflections corresponding to the superstructure and the observation of a pseudogap in the optical spectra at temperatures $T > T_{3D}$ [16, 20], as well as the CDW fluctuations, which are directly observed in femtosecond spectroscopy experiments [22].

There are quite a large number of theoretical studies in which the authors try to explain the observed anomalies. We can distinguish two main areas of these investigations. One of them is based on the formation of polarons in which the shift and smearing of the maximum of the density of states are explained in the framework of the polaron theory; i.e., mobile polarons with small coherence length are considered as quasiparticles. The interaction with phonons increases the effective mass of a carrier and gives rise to harmonics near the quasiparticle peak at E_F, instead of a typical Lorentzian, as well as leads to the smearing and shift of the quasiparticle peak by $\langle n_{ph}\rangle\hbar\omega$, where $\langle n_{ph}\rangle$ is the

average number of phonons interacting with electrons and $\hbar\omega$ is the characteristic phonon energy. However, the recent studies of $K_{0.3}MoO_3$ [23], where a quasiparticle peak with fine structure was obtained at 80 K with a resolution of about 1 meV, have shown that these features, as well as the small coherence length of quasiparticles recovered from the k dispersion, are better described by the so-called theoretical "ladder" model, in which electron–electron interactions are essential and in the framework of which the bound states due to the presence of spin and holon excitations are responsible for the peak. Features inherent in these excitations in the ARPES spectra are smeared due to Gaussian fluctuations and the fluctuations of the CDW wave vector on the crystal surface. At the same time, in $(TaSe_4)_2I$, EPI remains essential, and the CDW gap is likely to open against the background of the polaron gap, which exists at temperatures above T_P [24].

Another direction suggests that the pseudogap phenomena are mainly attributed to CDW-type short-range-order fluctuations. Quite a long time ago, Sadovskii proposed an exactly solvable model for the formation of a pseudogap in a 1D system due to developed short-range-order fluctuations of the CDW or the spin density wave (SDW) type [25–27]. This model stems directly from [21] and is of interest in connection with attempts to explain the pseudogap state of HTSC cuprates [28–30]. In particular, in [28–30], a significant generalization of this model was made to the case of a 2D electronic system in a random field of developed spin fluctuations (of antiferromagnetic short-range order).

As a rule, following Brazovskii [31, 32], one considers the effect of thermodynamic fluctuations of the order parameter on the Peierls gap in q1D systems similar to the effect of static disorder—by introducing a random potential with a Gaussian white noise type distribution. Brazovskii was the first who obtained the smearing of optical spectra, bound soliton states, and some other features.

2. P-GTB METHOD

In the cases of weak and strong electron–phonon coupling, one can apply perturbation theory with respect to EPI and electron hopping, respectively. In the first case, a large-radius polaron is formed, and the most accurate approach is that consisting in using a self-consistent Born approximation to calculate the self-energy part of the electron Green's function. In the second case, one applies the strong-coupling polaron theory or the theory of small-radius polarons and the Lang–Firsov canonical transformation [33]. These methods are well studied and provide controlled approximations. In the case of an intermediate EPI, analytical calculations based on perturbation theory become impossible. Therefore, increasing interest has recently been shown in nonperturbative methods such as the diagrammatic Monte Carlo method [34–36], the method of exact diagonalization of small clusters [37], variational methods [38], and the density matrix renormgroup method [39].

In the present study, we are not going to use perturbation theory with respect to EPI; instead, we consider the cases of strong and weak EPI within the generalized tight binding (GTB) method [40]. The advantage of this method is that it allows one to consider the cases of weak, strong, and intermediate EPI within the same approach. Moreover, the method allows one to calculate the electronic structure at various temperatures. Originally, the GTB method and its first-principles version LDA + GTB were proposed to describe the electronic structure of cuprates—high-temperature superconductors and various Mott–Hubbard systems—and are, in fact, an implementation of the cluster perturbation theory in terms of Hubbard's X operators. The results of calculations by the GTB method quantitatively depend on the set of microscopic parameters used, such as hopping integrals t. Using LDA wave functions for calculating Wannier functions by the projection technique [41], one can calculate the parameters of an appropriate model based on the real crystalline structure of the systems under test and thus relate the model approach to the characteristic features of real chemical compounds. In [42], the authors proposed a polaron version of the GTB (P-GTB) to calculate the electronic structure of strongly correlated systems with strong EPI. In this approach, one can distinguish three main stages.

(1) Decomposition of an infinite crystal lattice into a set of unit cells (clusters); in our case of the one-dimensional chain, these are clusters with two atoms. Exact diagonalization of the intracell Hamiltonian with regard to EPI and determination of the energy E_p and the multiparticle wave functions $|p\rangle$ of local polarons.

(2) Construction of polaron Hubbard's X operators $X_f^{pq} = |p\rangle\langle q|$ on the basis of local multielectron and multiphonon eigenstates from Section 1. The indices p and q include a set of quantum numbers that characterize the state of the system. The calculation of the matrix elements of the creation and annihilation operators of electrons and phonons in this basis allows one to express single-electron and phonon operators at a site as a liner combination of Hubbard's operators, which are quasi-Fermi for electrons and quasi-Bose for phonons.

(3) In the general case, a multiband model with electron–electron and electron–phonon interactions is expressed as a generalized Hubbard model in the representation of X operators with a set of local polaron states and the intercell hopping and interaction between them. The X operator representation allows one to take into account strong correlations and EPI in the first approximation of the theory. The band structure of quasiparticle excitations is formed due to intercell hopping, the conduction band (valence band)

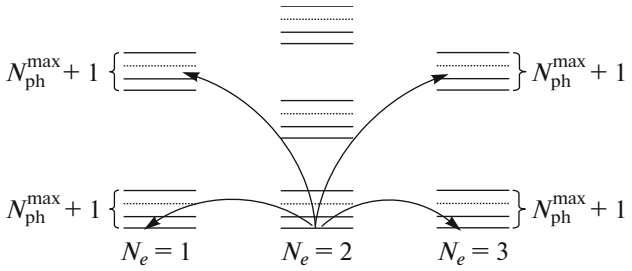

Fig. 1. Schematic view of multielectron vibronic energy levels of the eigenstates of a cluster with $N_e = 1, 2, 3$ electrons and Fermi excitations between these levels (arrows).

being attributed to the dispersion of Fermi excitations between multiparticle states with N_e and $N_e + 1$ ($N_e - 1$) electrons (Fig. 1).

An important new aspect of the theory developed is the dependence of the dispersion laws of quasiparticles on the occupation numbers of local states. In our case, temperature changes the occupation numbers of different multielectron terms and the occupation numbers of multiphonon levels, which may lead to a strong dependence of the dispersion laws of polarons on temperature.

3. MINIMAL MODEL

In the Peierls transition due to EPI, not only the electronic, but also the phonon system is rearranged (Kohn anomaly); therefore, a consistent analysis of the Peierls transition requires the introduction of a Hamiltonian describing electrons, phonons, and their interaction.

In the strong-coupling model, one can assume that the displacement of ions from equilibrium position changes only resonance integrals t (hopping integrals). Therefore, the electron Hamiltonian with regard to the motion of ions is given by

$$H = \sum_i \frac{p_i^2}{2M} + \frac{1}{4} M\omega_0^2 \sum_i (u_{i+1} - u_i)^2 - t\sum_{i,\sigma} (a_{i+1,\sigma}^\dagger a_{i,\sigma} + a_{i,\sigma}^\dagger a_{i+1,\sigma}) + t' \sum_{i,\sigma} (u_{i+1} - u_i)(a_{i+1,\sigma}^\dagger a_{i,\sigma} + a_{i,\sigma}^\dagger a_{i+1,\sigma}), \quad (1)$$

where p_i and u_i are the momentum and displacement operators of an atom at site i, t' is the derivative of the resonance integral with respect to the interatomic distance, and M is the ion mass. Further, one usually passes to the phonon representation and obtains a Fröhlich Hamiltonian; however, it is more convenient to deal with the representation of bare Einstein phonons. Let us introduce the creation and annihilation operators of an excitation quantum of the ith oscillator, i.e., $b_i^\dagger$ and b_i:

$$u_i = \sqrt{\frac{1}{2M\omega_0}}(b_i + b_i^\dagger), \quad p_i = \frac{1}{i}\sqrt{\frac{M\omega_0}{2}}(b_i - b_i^\dagger).$$

As a result, we obtain

$$H = \omega_0 \sum_i \left(b_i^\dagger b_i + \frac{1}{2}\right) - \frac{\omega_0}{4}\sum_i (b_i + b_i^\dagger) \times (b_{i+1} + b_{i+1}^\dagger) - t\sum_{\langle ij\rangle,\sigma} a_{i,\sigma}^\dagger a_{j,\sigma} + \sum_{i,\langle jk\rangle,\sigma} (\lambda_{0jk}^i b_i^\dagger + \lambda_{0kj}^{*i} b_i) a_{j,\sigma}^\dagger a_{k,\sigma}, \quad (2)$$

where λ_0 is the EPI parameter. Below, we will use, as customary, a dimensionless EPI parameter $\lambda = \lambda_0^2/zt\omega_0$, where z is the number of nearest neighbors, and distinguish the cases of weak ($\lambda = 0.02$) and strong ($\lambda = 0.4$) EPI.

Let us decompose the one-dimensional chain into a set of elementary cells (clusters) with two neighboring atoms in a cell. Then expression (2) is rewritten as

$$H = H_C + H_{CC}, \quad (3)$$

where H_C and H_{CC} are the intracell and intercell parts of the Hamiltonian (2), respectively:

$$H_C = H_C^e + H_C^{ph} + H_C^{e-ph} + H_C^{ph-ph}, \quad (4)$$

$$H_{CC} = H_{CC}^e + H_{CC}^{e-ph} + H_{CC}^{ph-ph}. \quad (5)$$

Here

$$H_C^{ph} = \omega_0 \sum_f \sum_{l=1}^{2} \left(b_{f,l}^\dagger b_{f,l} + \frac{1}{2}\right)$$

is the energy of local oscillations in a cluster;

$$H_C^e = -t\sum_{f,\sigma} \sum_{l\neq l'} a_{f,l,\sigma}^\dagger a_{f,l',\sigma}$$

contains electron hopping in a cell;

$$H_C^{e-ph} = \lambda \sum_f \sum_{l\neq l'} [(b_{f,l}^\dagger + b_{f,l}) + (b_{f,l'}^\dagger + b_{f,l'})] a_{f,l,\sigma}^\dagger a_{f,l',\sigma}$$

and

$$H_C^{ph-ph} = -\frac{\omega_0}{4}\sum_f \sum_{l\neq l'} b_{f,l}^\dagger b_{f,l'} - \frac{\omega_0}{4}\sum_f (b_{f,1} b_{f,2} + b_{f,1}^\dagger b_{f,2}^\dagger)$$

are intracell parts of the electron–phonon and phonon–phonon interactions, respectively;

$$H_{CC}^{e} = \sum_{\langle fg\rangle,\sigma}\sum_{l\neq l'} t_{fg}^{ll'} a_{f,l,\sigma}^{\dagger} a_{g,l',\sigma}$$

describes intercluster electron hopping; and $H_{CC}^{\mathrm{e-ph}}$ and $H_{CC}^{\mathrm{ph-ph}}$ are the intercell parts of the electron–phonon and phonon–phonon interactions, respectively. The index f numbers the position of a cell in the new superlattice, and $l = 1, 2$ is the position of an atom in a cell.

Single-electron and phonon annihilation and creation operators in a cell f with spin projection σ can be expressed as a linear combination of X operators, which are quasi-Fermi for electrons:

$$a_{f,\sigma} = \sum_{pq} |p\rangle\langle p|a_{f,\sigma}|q\rangle\langle q| = \sum_{pq} \gamma_{\sigma}(pq) X_f^{pq},$$

$$a_{f,\sigma}^{\dagger} = \sum_{m} \gamma_{\sigma}^{*}(pq) X_f^{\dagger pq}$$

and quasi-Bose for phonons:

$$b_f = \sum_{pp'} |p\rangle\langle p|b_f|p'\rangle\langle p'| = \sum_{pp'} \gamma(pp') X_f^{pp'},$$

$$b_f^{\dagger} = \sum_{pp'} \gamma^{*}(pp') X_f^{\dagger pp'},$$

where $|p\rangle$ and $|q\rangle$ are multielectron and multiphonon eigenstates of the intracell part of Hamiltonian (4) $H_C|p\rangle = E_p|p\rangle$ with different numbers of electrons $N_e = 1, 2$, or 3. In other words, since the number of different root vectors (pq) is finite, the vectors can be numbered, and each vector can be assigned a number m; then

$$a_{f,\sigma} = \sum_{m} \gamma_{\sigma}(m) X_f^{m}, \quad a_{f,\sigma}^{\dagger} = \sum_{m} \gamma_{\sigma}^{*}(m) X_f^{\dagger m}.$$

For $N_e = 1$, the set of eigen-wave functions $|p\rangle_i$, doubly degenerate with respect to the spin σ, can be represented as

$$|p\rangle_i = \sum_{n_{\mathrm{ph}}=0}^{N_{\mathrm{ph}}^{\max}} \sum_{l} c_l^i(n_{\mathrm{ph}})|a_{l,\sigma}\rangle|n_{\mathrm{ph}}\rangle,$$

where

$$|n_{\mathrm{ph}}\rangle = \frac{1}{\sqrt{n_{\mathrm{ph}}!}}(b^{\dagger})^{n_{\mathrm{ph}}}|0,0,\ldots,0\rangle$$

and

$$|a_{l,\sigma}\rangle = a_{l,\sigma}^{\dagger}|0\rangle,$$

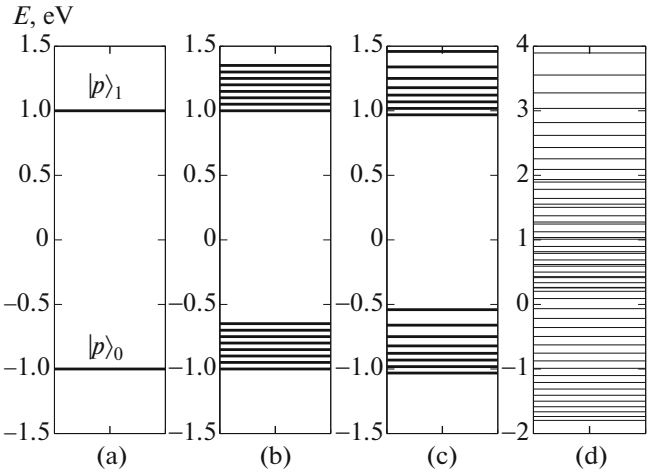

Fig. 2. Set of energy levels of eigenstates of a cluster with $N_e = 1$ electron for (a) $n_{\mathrm{ph}} = 0$, (b) $n_{\mathrm{ph}} = 7$, (c) for weak EPI with $n_{\mathrm{ph}} = 7$ and $\lambda = 0.04$, and (d) for strong EPI with $n_{\mathrm{ph}} = 30$ and $\lambda = 0.2$. Calculations are made for $t = 1$ eV and $\omega_0 = 0.05$ eV.

and $N_{\mathrm{ph}}^{\max}$ is the cutoff number of phonons starting from which, for $n_{\mathrm{ph}} > N_{\mathrm{ph}}^{\max}$ and a given value of EPI, the energy of the ground state $|p_0\rangle$,

$$E_p^0(N_{\mathrm{ph}}^{\max} + 1) \approx E_p^0(N_{\mathrm{ph}}^{\max})$$

and the weight coefficients

$$c_l^0(N_{\mathrm{ph}}^{\max} + 1) \approx c_l^0(N_{\mathrm{ph}}^{\max})$$

(when considering various temperature phenomena, one should track the invariance of the energy E_p^i of the nearest excited states $|p\rangle_i$ and the weight coefficients $c_l^i(N_{\mathrm{ph}}^{\max} + 1) \approx c_l^i(N_{\mathrm{ph}}^{\max})$) cease to change. In other words, $N_{\mathrm{ph}}^{\max}$ determines the number of phonons that should be taken into consideration for a given value of EPI in order that a "phonon dressing" of an electron be formed and a polaron be created. For $N_e = 2$, eigenstates can be represented, with regard to the Pauli principle, as a linear combination

$$|p\rangle_i = \sum_{n_{\mathrm{ph}}=0}^{N_{\mathrm{ph}}^{\max}} \sum_{ll',\sigma\sigma'} c_{ll',\sigma\sigma'}^{i}(n_{\mathrm{ph}})|a_{l,\sigma}a_{l',\sigma'}\rangle|n_{\mathrm{ph}}\rangle,$$

where

$$|a_{l,\sigma}a_{l',\sigma'}\rangle = a_{l,\sigma}^{\dagger}a_{l',\sigma'}^{\dagger}|0\rangle.$$

The maximum number of electrons in a cluster is $N_e^{\max} = 4$; therefore, for $N_e = 3$, the wave function in

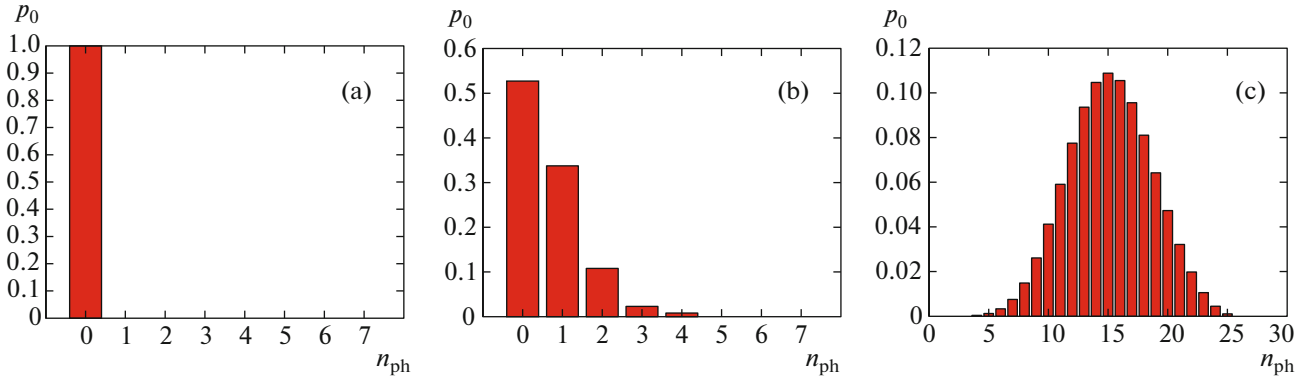

Fig. 3. (Color online) Histograms of the weight contribution of basis states with various numbers of phonons to the ground state of a cluster with $N_e = 1$ electron in the cases of (a) $n_{ph} = 0$ and $n_{ph} = 7$, $\lambda = 0$, (b) weak $n_{ph} = 7$ and $\lambda = 0.02$, and (c) strong $n_{ph} = 30$ and $\lambda = 0.4$ EPI. Calculations are made for $t = 1$ eV and $\omega_0 = 0.05$ eV.

the hole representation has a form analogous to that for $N_e = 1$.

Figure 2 demonstrates, as an example, a set of energy levels of eigenstates of a cluster with $N_e = 1$ for three possible cases:

(1) $n_{ph} = 0$. In the absence of local oscillations, there are only two electron states that are doubly degenerate with respect to the spin projection σ: the ground state

$$|p\rangle_0 = \frac{1}{\sqrt{2}}(a^\dagger_{1,\sigma} - a^\dagger_{2,\sigma})|0\rangle$$

and the excited state

$$|p\rangle_1 = \frac{1}{\sqrt{2}}(a^\dagger_{1,\sigma} + a^\dagger_{2,\sigma})|0\rangle$$

(Fig. 2a);

(2) $n_{ph} = 7$ and $\lambda = 0$. In the presence of local oscillations but in the absence of EPI, there is an equidistant spectrum for the ground $|p\rangle_0$ and excited $|p\rangle_1$ electronic states (Fig. 2b);

(3) the case of a weak, $n_{ph} = 7$ and $\lambda = 0.02$ (Fig. 2c), and strong, $n_{ph} = 30$ and $\lambda = 0.4$ (Fig. 2d), EPI.

Figure 3 demonstrates the histogram of the distribution of the weight contribution

$$P_0 = \sum_l |c^0_l(n_{ph})|^2$$

of the basis states $|a_{l,\sigma}\rangle|n_{ph}\rangle$ with different numbers of phonons to the ground state $|p\rangle_0$ in cases (1) and (2) of (a, b) weak and (c) strong EPI. One can see that, as the value of EPI increases, the contribution of basis states with a greater number of phonons increases, while the fraction of pure electronic states, conversely, decreases. Such a redistribution of weight leads to the situation that Fermi excitations between multiparticle states with N_e and $N_e + 1$ ($N_e - 1$) electrons (Fig. 1) acquire a satellite structure, so that the specific weight Z of the quasiparticle peak decreases, while the specific contribution of a noncoherent phonon to the total spectral weight, conversely, increases. Band broadening takes place with stronger energy smearing of quasiparticle peaks in the ARPES spectra.

Without taking into account the intercell electron–phonon H_{CC}^{e-ph} and phonon–phonon H_{CC}^{ph-ph} interactions, Hamiltonian (3) in the representation of X operators takes the form

$$H = \sum_{f,p} E_p X^{pp}_f + \sum_{f\neq g}\sum_{m,n} t^{mn}_{fg} X^{\dagger m}_f X^n_g, \qquad (6)$$

where

$$t^{mn}_{fg} = \sum_\sigma t_{fg}\gamma^*_\sigma(m)\gamma_\sigma(n)$$

contains intercluster hopping integrals t_{fg}.

To obtain the dispersion relations for quasiparticle excitations, we apply the method of equations of motion for the matrix Green's function of polarons:

$$D_{mn}(k,\omega) = \langle\langle X^m_k | X^{\dagger n}_k\rangle\rangle,$$

which is related to the single-electron Green's function

$$G_\sigma(k,\omega) = \langle\langle a_{k\sigma}|a^\dagger_{k\sigma}\rangle\rangle$$

by the formula

$$G_\sigma(k,\omega) = \sum_{m,n}\gamma_\sigma(m)\gamma^*_\sigma(n)D_{mn}(k,\omega).$$

The spectral density of single-particle excitations

$$A_\sigma(k,\omega) = -\frac{1}{\pi}\sum_{mn}\gamma_\sigma(m)\gamma^*_\sigma(n)$$

$$\times \mathrm{Im}\, D_{mn}(k,\omega + i\delta) = -\frac{1}{\pi}\mathrm{Im}\, G(k,\omega + i\delta)$$

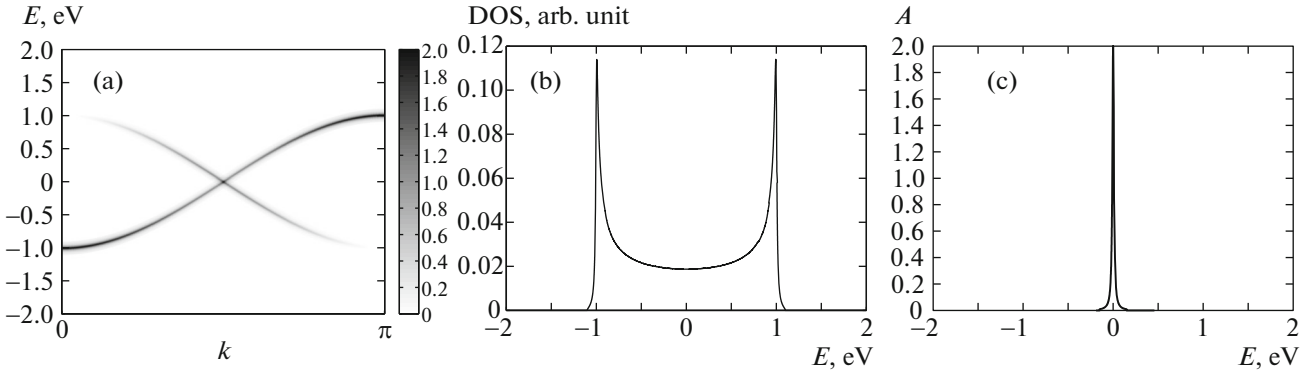

Fig. 4. Electronic structure (band structure, density of states, and the spectral density at the point with the wave vector $k = \pi/2$ at the chemical potential level) in the absence of EPI. All calculations are performed for the following values of the parameters: $\lambda = 0$, $t = 1$ eV, and $\delta = 0.03$ eV.

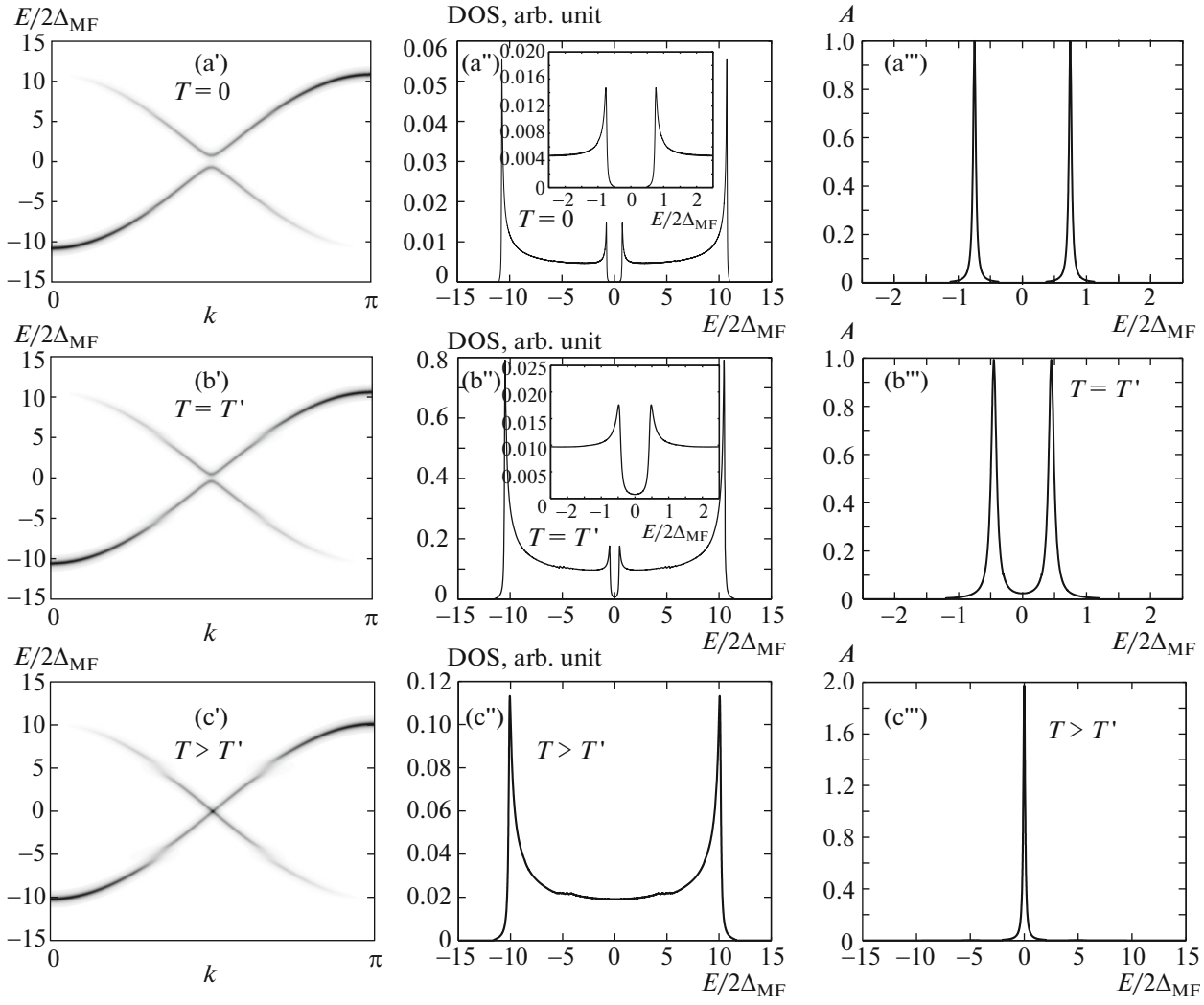

Fig. 5. Electronic structure (band structure, density of states, and the spectral density at the point with the wave vector $k = \pi/2$ at the chemical potential level) in the case of a weak EPI calculated for three values of temperature: (a) $T = 0$, (b) $T = T'$, and (c) $T > T'$. All calculations are performed for the following values of parameters: $\omega_0 = 0.05$ eV, $\lambda = 0.02$, $t = 1$ eV, and $\delta = 0.02–0.05$ eV.

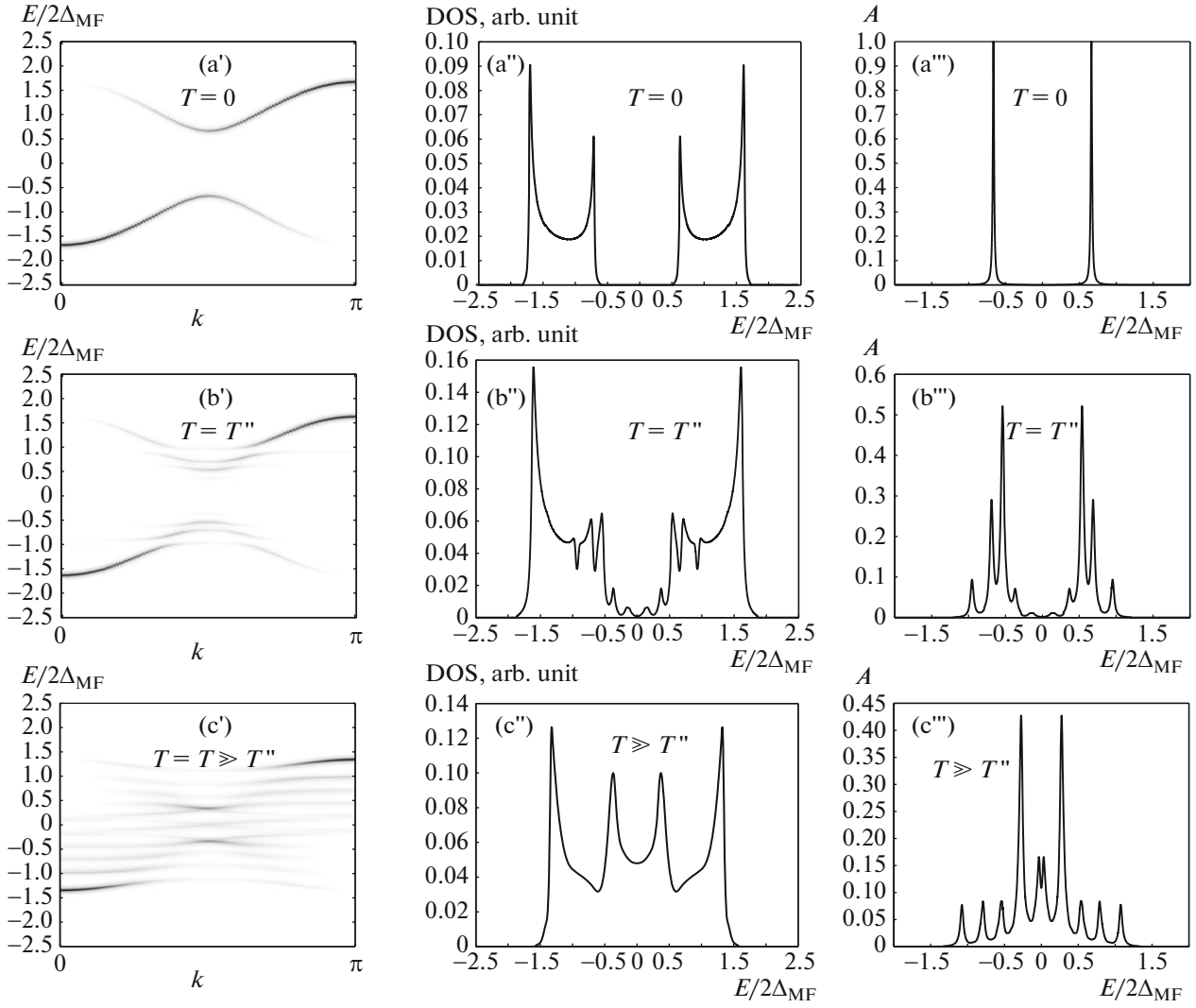

Fig. 6. Electronic structure (band structure, density of states, and the spectral density at the point with the wave vector $k = \pi/2$ at the chemical potential level) in the case of a strong EPI calculated for three values of temperature: (a) $T = 0$, (b) $T = T''$, and (c) $T \gg T''$. All calculations are performed for the following values of parameters: $\omega_0 = 0.05$ eV, $\lambda = 0.4$, $t = 1$ eV, and $\delta = 0.02$–0.05 eV.

and the density of single-particle states for a given spin projection (N_k is the normalization factor)

$$N_\sigma(\omega) = \frac{1}{N_k}\sum_k A_\sigma(k,\omega)$$

are expressed in terms of the Fermi single-particle Green's function.

For the Green's function $\hat{D}$, we can write a generalized Dyson equation [42, 43]

$$\hat{D}_k(\omega) = [\hat{G}_0^{-1}(\omega) - \hat{P}_k(\omega)(\hat{t}_k + \hat{\Lambda}_k) + \hat{\Sigma}_k(\omega)]\hat{P}_k(\omega). \quad (7)$$

Here, $\hat{\Sigma}_k(\omega)$ and $\hat{P}_k(\omega)$ are the mass and strength operators, respectively, $\hat{G}_0(\omega)$ is a local intracell propagator, and

$$\hat{t}_k^{mn} = \sum_\sigma \gamma_\sigma^*(m)\gamma_\sigma(n)t_k,$$

where t_k is the Fourier transform of intercluster hopping.

The similarity between (6) and the Hamiltonian of the Hubbard model in the X operator representation allows one to apply many perturbation theory methods known for the Hubbard model. In the Hubbard-I approximation, the structure of exact Green's function (7) is preserved, the mass operator is set equal to zero, and the strength operator is

$$\hat{P}_k^{mn}(\omega) = \delta_{mn}F_m,$$

where

$$F_m \equiv F(pq) = \langle X^{pp}\rangle + \langle X^{qq}\rangle$$

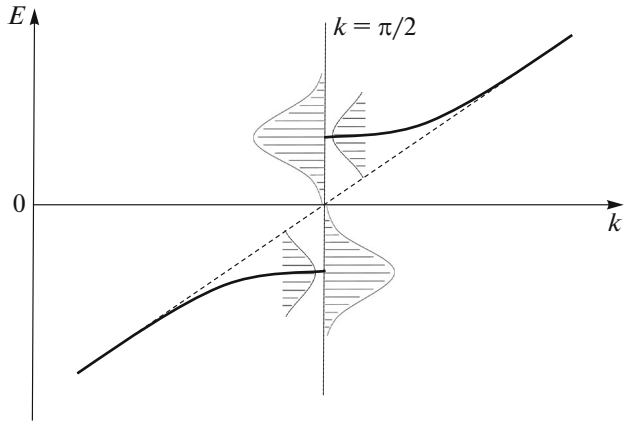

Fig. 7. Schematic illustration of the formation of a pseudogap state as a result of a strong EPI. The dashed line shows the location of a coherent quasiparticle peak. The solid line shows the position of the intensity maximum of the APRES spectrum.

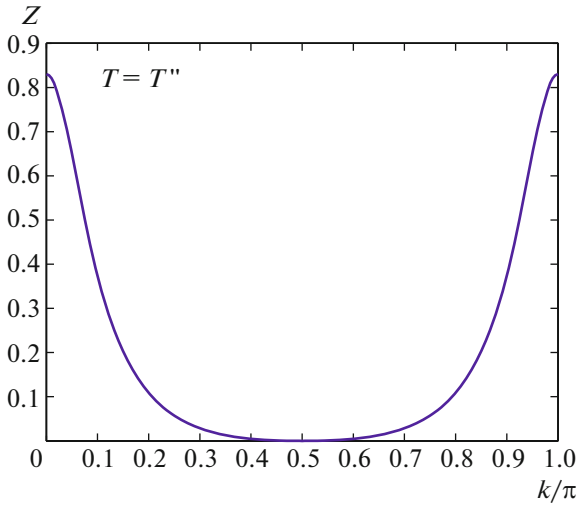

Fig. 8. (Color online) Specific weigh Z of a quasiparticle peak as a function of a wave vector k in the case of a strong EPI. Calculations are performed for the following values of parameters: $\omega_0 = 0.05$ eV, $\lambda = 0.4$, and $t = 1$ eV.

is a filling factor, called the end factor in the diagram technique for X operators [44]. From Eq. (7) we obtain

$$\hat{D}_k^{-1} = \hat{D}_0^{-1} + \hat{t}_k.$$

Here

$$\hat{D}_0^{mn} = \delta_{mn} F_m/(\omega - \Omega_m),$$

where

$$\Omega_m \equiv \Omega(pq) = E_p - E_q.$$

The dispersion relation of Fermi quasiparticles is determined by the equation for the poles of the matrix Green's function $\hat{D}_k$:

$$\det \|\delta_{mn}(\omega - \Omega_m)/F_m - t^{mn}(k)\| = 0. \qquad (8)$$

This equation has a form similar to the dispersion equation of the strong-coupling method in single-electron bandgap theory but differs from the latter in two respects: first, the indices m and n number single-particle excitations in the multielectron and multiphonon systems, respectively, rather than single-electron orbitals, and, second, the effective hopping integral is determined by the product of $t^{mn}(k)$ and the filling factor F_m, which depends on the occupation numbers of the initial and finals states (Fig. 1). As a result, the band structure of quasiparticles depends on temperature, in contrast to the single-electron band structure.

4. BAND STRUCTURE OF POLARONS WITHIN CLUSTER PERTURBATION THEORY P-GTB

The cluster perturbation theory has been successfully applied to the analysis of the Hubbard model [45, 46] and is exact in the limit of electron–electron interaction $U = 0$ and $U \to \infty$. In our case, we do not consider electron correlations, and precisely the first variant is implemented; therefore, we do not face the problems associated with the artificial period-doubling of the crystalline lattice. This is clearly seen in Fig. 4, which demonstrates the results of our cluster calculation in the absence if EPI. For $\lambda = 0$, Hamiltonian (2) is exactly diagonalized by passing to the k-space. The electronic band structure exhibits typical metallic behavior, and, as is obvious, no dips associated with the artificial period-doubling of the one-dimensional chain of atoms arise in the density of states (Fig. 4b); the spectral density $A(k, \omega)$ at the point with wave vector $k = \pi/2$ at the chemical potential level manifests itself by a Lorentzian peak (Fig. 4c). The band structure is independent of temperature.

If a long-range order arises in the system (for example, of SDW or CDW type), a (dielectric) gap opens in the spectrum of elementary excitations. For instance, in our example, at $T = 0$ and $\lambda \neq 0$, a gap $E_g = 2\Delta$ opens in the energy spectrum at the Fermi level (Figs. 5a and 6a). The system becomes dielectric. The width of the gap is determined by the value of EPI. In the cases of weak and strong EPI, two peaks arise in the spectral density, which correspond to "Bogolyubov" quasiparticles (Figs. 5a''' and 6a'''). Thus, the ground state of the system has qualitatively the same form irrespective of the value of EPI—the dielectric gap is attributed to the CDW-type long-range order.

However, as temperature increases, these two cases exhibit essentially different behavior. In the case of weak EPI, the spectral weights of the two peak overlap at $T = T'$ (Fig. 5b''') and, for $T > T'$, they merge

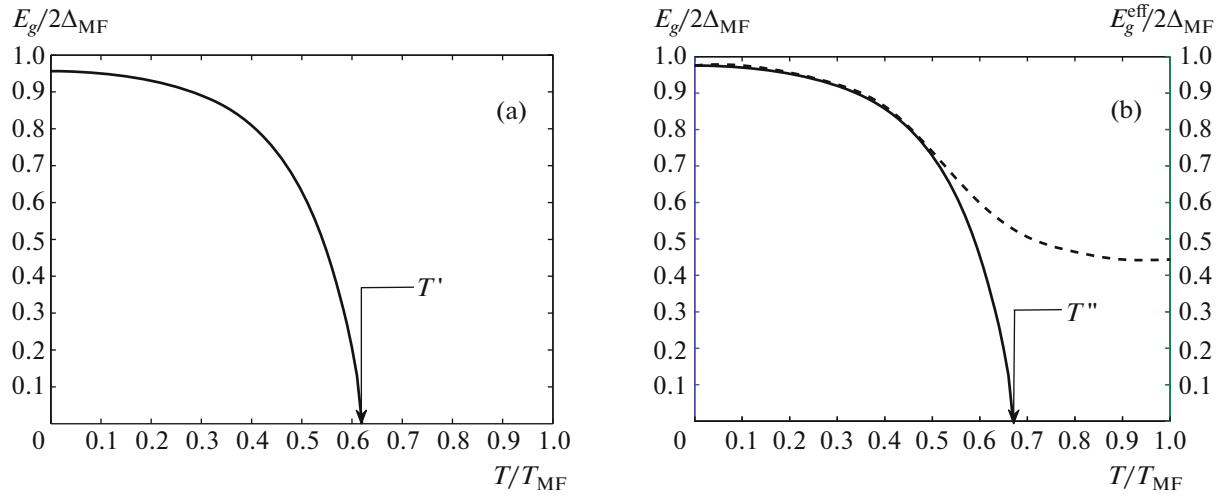

Fig. 9. Temperature dependence of the dielectric gap E_g (solid line) and the effective gap E_g^{eff} (dashed line) in the cases of (a) weak and (b) strong EPI; $2\Delta_{MF}$ and T_{MF} are the gap and the transition temperature in the mean field theory.

together into a single Lorentzian peak (Fig. 5c'''), which is characteristic of a normal metal (a Fermi liquid), and the dielectric gap in the density of states slowly disappears (Figs. 5b'' and 5c'').

A qualitatively different variation in the band structure with increasing temperature can be observed in the case of strong EPI. Figures 6b and 6c demonstrate the main polaron effect—the splitting of bands into polaron subbands and the formation of polarons themselves—Fermi-type excitations in the system that are a manifestation of a hybridized state of Fermi-type quasiparticles and local multiphonon Frank–Condon resonances [47, 48]. A significant renormalization of single-particle excitations occurs due to the strong EPI. Considerable part of spectral weight is redistributed between a coherent peak of quasiparticle excitations and the noncoherent part of the spectrum that is located at lower energy and is attributed to the emergence of vibronic satellites. At some temperature $T = T''$, the spectral weights of two peaks overlap (Fig. 6b'''); however, due to the strong decrease in the spectral weight of the coherent quasiparticle peak, a so-called hidden Fermi surface opens. Since in ARPES experiments one directly measures the product $f(\omega)A(k,\omega)$, where $f(\omega) = [\exp(\omega/T) + 1]^{-1}$ is the Fermi distribution function, characteristic features of the intensity spectra of an ARPES signal for q1D compounds with CDWs are the shift of the maximum intensity into the band gap away from the Fermi level and its broadening with stronger (Gaussian) energy smearing compared with that for ordinary quasiparticles in three-dimensional metals at the Fermi level, for which the maximum is described by a Lorentzian. Schematically, this situation is illustrated in Fig. 7; Fig. 8 demonstrates the calculated specific weight Z of the quasiparticle peak as a function of the wave vector k in the case of a strong EPI for $T = T''$. In spite of the fact that the system passes to the metallic state for $T > T''$, a dip in the density of states remains even at high temperatures $T \gg T''$ (Fig. 6c''). All the calculations have been made in the Hubbard-I approximation to exclude the damping of quasiparticle excitations and smearing of the gap with increasing temperature.

The solid line in Fig. 9 shows the temperature dependence of $E_g/2\Delta_{MF}$, where $2\Delta_{MF}$ is the gap width in the mean field theory as a function of normalized temperature T/T_{MF} in the cases of weak (a) and strong (b) EPI. One can see that T' an T'' are less than T_{MF}. The dashed curve in Fig. 9b demonstrates the behavior of the effective gap $E_g^{\text{eff}}/2\Delta_{MF}$, which is determined at a level where the density of states is e times greater than the density of states at the Fermi level: $\text{DOS}(E_g^{\text{eff}}/2) = e\text{DOS}(0)$. It is clear that the gap E_g^{eff} exists in the spectrum for arbitrarily high temperatures and, as temperature increases, reaches a constant value approximately equal to $E_g(0)/2$. Such behavior well agrees with the results of [49], where the authors experimentally determined a certain effective gap Δ_{eff} in the spectrum of $K_{0.3}MoO_3$, which exists for $T > T_P$.

5. CONCLUSIONS

On the basis of the calculations and the comparison of two limit cases of EPI, we can conclude that the ground state of quasi-one-dimensional systems has qualitatively the same form irrespective of the electron–phonon interaction—the dielectric gap is attributed to CDW-type long-range order. In q1D systems with strong EPI, along with a CDW gap, which is

responsible for the dielectric ground state, there exists a polaron gap, or a gap of polaron origin, which is responsible for the pseudogap behavior of these gaps with increasing temperature.

In addition to q1D compounds, pseudogap phenomena are observed in manganites with colossal magnetoresistance and in HTSC cuprates. The nature of this phenomenon within the polaron approach has remained the subject of constant discussions [50–57]. In the present study, we have presented a theoretical calculation that confirms the statements made above.

ACKNOWLEDGMENTS

This work was supported by the Russian Foundation for Basic Research (project nos. 17-02-00826, 16-02-00507, 16-02-00098, and 16-02-00273), by the Government of the Krasnoyarsk krai, by the Krasnoyarsk Regional Foundation for Supporting Scientific and Technological Activity (project nos. 16-42-243048, 16-42-240746, and 16-43-240505)), and by the Grants Council of the President of the Russian Federation (project nos. SP-1844.2016.1 and NSh-7559.2016.2).

REFERENCES

1. I. Bloch, Nat. Phys. **1**, 23 (2005).
2. E. Pazy and A. Vardi, Phys. Rev. A **72**, 033609 (2005).
3. U. Bissbort, D. Cocks, A. Negretti, Z. Idziaszek, T. Calarco, F. Schmidt-Kaler, W. Hofstetter, and R. Gerritsma, Phys. Rev. Lett. **111**, 080501 (2013).
4. M. Bruderer, A. Klein, S. R. Clark, and D. Jaksch, Phys. Rev. A **76**, 011605(R) (2007).
5. C. Kohstall, M. Zaccanti, M. Jag, A. Trenkwalder, P. Massignan, G. M. Bruun, F. Schreck, and R. Grimm, Nature **485**, 615 (2012).
6. L. N. Bulaevskii, Sov. Phys. Usp. **18**, 131 (1975).
7. R. E. Peierls, *Quantum Theory of Solids* (Oxford Univ. Press, Oxford, 1955).
8. E. H. Lieb and F. Y. Wu, Phys. Rev. Lett. **20**, 1445 (1968).
9. N. F. Mott and W. D. Twose, Adv. Phys. **10**, 107 (1961).
10. V. L. Berezinskii, Sov. Phys. JETP **38**, 620 (1973).
11. V. Ya. Pokrovskii, S. G. Zybtsev, M. V. Nikitin, I. G. Gorlova, V. F. Nasretdinova, and S. V. Zaitsev-Zotov, Phys. Usp. **56**, 29 (2013).
12. S. V. Zaitsev-Zotov, Phys. Usp. **47**, 533 (2004).
13. M. Grioni, S. Pons, and E. Frantzeskakis, J. Phys.: Condens. Matter **21**, 023201 (2009).
14. L. Perfetti, S. Mitrovic, G. Margaritondo, M. Grioni, L. Forro, L. Degiorgi, and H. Hochst, Phys. Rev. B **66**, 075107 (2002).
15. L. Perfetti, H. Berger, A. Reginelli, L. Degiorgi, H. Hochst, J. Voit, G. Margaritondo, and M. Grioni, Phys. Rev. Lett. **87**, 216404 (2001).
16. P. Monceau, Adv. Phys. **61**, 325 (2012).
17. F. Ya. Nad' and M. E. Itkis, JETP Lett. **63**, 262 (1996).
18. K. Kim, R. H. McKenzie, and J. W. Wilkins, Phys. Rev. Lett. **71**, 4015 (1993).
19. S. Brown and A. Zettl, in *Charge Density Waves in Solids*, Vol. 25 of *Modern Problems in Condensed Matter Science*, Ed. by L. P. Gor'kov and G. Gruner (North-Holland, Amsterdam, 1989), p. 223.
20. G. Gruner, *Density Waves in Solids* (Addison-Wesley, Reading, MA, 1994).
21. P. A. Lee, T. M. Rice, and P. W. Anderson, Phys. Rev. Lett. **31**, 462 (1973).
22. R. Yusupov, T. Mertelj, V. V. Kabanov, S. Brazovskii, P. Kusar, J.-H. Chu, I. R. Fisher, and D. Mihailovic, Nat. Phys. **6**, 681 (2010).
23. D. Mou, R. M. Konik, A. M. Tsvelik, I. Zaliznyak, and X. Zhou, Phys. Rev. B **89**, 201116(R) (2014).
24. C. Tournier-Colletta, L. Moreschini, G. Autes, S. Moser, A. Crepaldi, H. Berger, A. L. Walter, K. S. Kim, A. Bostwick, P. Monceau, E. Rotenberg, O. V. Yazyev, and M. Grioni, Phys. Rev. Lett. **110**, 236401 (2013).
25. M. V. Sadovskii, Sov. Phys. JETP **39**, 845 (1974).
26. M. V. Sadovskii, Sov. Phys. Solid State **16**, 1632 (1974).
27. M. V. Sadovskii, Sov. Phys. JETP **50**, 989 (1979).
28. J. Schmalian, D. Pines, and B. Stojkovic, Phys. Rev. Lett. **80**, 3839 (1998).
29. J. Schmalian, D. Pines, and B. Stojkovic, Phys. Rev. B **60**, 667 (1999).
30. E. Z. Kuchinskii and M. V. Sadovskii, J. Exp. Theor. Phys. **88**, 968 (1999).
31. S. A. Brazovskii, JETP Lett. **28**, 606 (1978).
32. S. A. Brazovskii, I. E. Dzyaloshinskii, and S. P. Obukhov, Sov. Phys. JETP **45**, 814 (1977).
33. I. G. Lang and Yu. A. Firsov, Sov. Phys. JETP **16**, 1301 (1963).
34. N. Prokof'ev and B. Svistunov, Phys. Rev. Lett. **81**, 2514 (1998).
35. A. Mishchenko, N. Prokof'ev, A. Sakamoto, and B. Svistunov, Phys. Rev. B **62**, 6317 (2000).
36. P. E. Kornilovitch, Phys. Rev. Lett. **81**, 5382 (1998).
37. A. S. Alexandrov, Phys. Rev. B **49**, 9915 (1994).
38. V. Cataudella, G. D. Filippis, and G. Iadonisi, Phys. Rev. B **62**, 1496 (2000).
39. E. Jeckelmann and S. R. White, Phys. Rev. B **57**, 6367 (1998).
40. S. G. Ovchinnikov, V. A. Gavrichkov, M. M. Korshunov, and E. I. Shneyder, Springer Ser. Solid-State Sci. **171**, 143 (2012).
41. V. I. Anisimov, D. E. Kondakov, A. V. Kozhevnikov, I. A. Nekrasov, Z. V. Pchelkina, J. W. Allen, S.-K. Mo, H.-D. Kim, P. Metcalf, S. Suga, A. Sekiyama, G. Keller, I. Leonov, X. Ren, and D. Vollhardt, Phys. Rev. B **71**, 125119 (2005).
42. I. A. Makarov, E. I. Shneyder, P. A. Kozlov, and S. G. Ovchinnikov, Phys. Rev. B **92**, 155143 (2015).
43. S. G. Ovchinnikov and V. V. Val'kov, *Hubbard Operators in the Theory of Strongly Correlated Electrons* (Imperial College, London, Singapore, 2004).
44. R. O. Zaitsev, Sov. Phys. JETP **43**, 574 (1976).
45. D. Senechal, A.-M. Tremblay, and C. Bourbonnais, *Theoretical Methods for Strongly Correlated Electrons* (Springer, Berlin, Heidelberg, 2004).

46. S. V. Nikolaev and S. G. Ovchinnikov, J. Exp. Theor. Phys. **111**, 635 (2010).

47. G. A. Sawatzky, Nature (London) **342**, 480 (1989).

48. G. D. Mahan, *Many Particle Physics* (Plenum, New York, 1990).

49. D. C. Johnston, Phys. Rev. Lett. **52**, 2049 (1984).

50. D. S. Dessau, T. Saitoh, C.-H. Park, Z.-X. Shen, P. Villella, N. Hamada, Y. Moritomo, and Y. Tokura, Phys. Rev. Lett. **81**, 192 (1998).

51. N. Mannella, W. L. Yang, X. J. Zhou, H. Zheng, J. F. Mitchell, J. Zaanen, T. P. Devereaux, N. Nagaosa, Z. Hussain, and Z.-X. Shen, Nature **438**, 474 (2005).

52. D. S. Marshall, D. S. Dessau, A. G. Loeser, C.-H. Park, A. Y. Matsuura, J. N. Eckstein, I. Bozovic, P. Fournier, A. Kapitulnik, W. E. Spicer, and Z.-X. Shen, Phys. Rev. Lett. **76**, 4841 (1996).

53. A. G. Loeser, Z.-X. Shen, D. S. Dessau, D. S. Marshall, C. H. Park, P. Fournier, and A. Kapitulnik, Science **273**, 325 (1996).

54. H. Ding, T. Yokoya, J. C. Campuzano, T. Takahashi, M. Randeria, M. R. Norman, T. Mochiku, K. Kadowaki, and J. Giapintzakis, Nature (London) **382**, 51 (1996).

55. Udai Raj Singh, S. Chaudhuri, R. C. Budhani, and Anjan K. Gupta, J. Phys.: Condens. Matter **21**, 355001 (2009).

56. A. Bussmann-Holder, H. Keller, A. R. Bishop, A. Simon, and K. A. Muller, J. Supercond. Novel Magn. **21**, 353 (2008).

57. G. Sica, J. H. Samson, and A. S. Alexandrov, Europhys. Lett. **100**, 37005 (2012).

Translated by I. Nikitin